

Translationally hot neutrals in etching discharges

Timothy J. Sommerer and Mark J. Kushner

University of Illinois, Department of Electrical and Computer Engineering, 1406 West Green Street, Urbana, Illinois 61801

(Received 30 January 1991; accepted for publication 29 April 1991)

The presence and influence of translationally energetic ions in low-pressure etching discharges is well known. Neutral atoms and molecules, though known to be chemically reactive, are not generally considered to be otherwise activated in these plasmas. Neutral species may, however, become translationally hot through either charge exchange collisions or by dissociative excitation caused by electron impact. These species are important in etching discharges because they may bring an isotropic source of activation energy to the substrate which may compromise anisotropic etching mechanisms. In this paper we present a theoretical study of the sources and effects of translationally hot neutral atoms and molecules in CF_4 etching plasmas. We find that ballistically hot F atoms comprise a significant fraction of the radical flux striking the substrate at pressures of < 100 mTorr. In CF_4 plasmas, the maximum flux of translationally hot F incident on the substrate of a parallel-plate rf etching discharge occurs between 10 and 100 mTorr. At these pressures the hot atom and ion fluxes to the substrate are comparable. The effects of translationally hot species on gas-phase plasma chemistry and surface reactions are discussed.

I. INTRODUCTION

Plasma etching of semiconductor materials is now the accepted method of fabricating micrometer and submicrometer features for very-large-scale integrated circuits.¹ A desirable feature of plasma etching is that highly anisotropic structures can be fabricated, an example being a deep trench with a large aspect ratio and nearly vertical walls. The ability to fabricate these structures rests on a number of effects working in concert, the details of which vary with the particular chemistry being used. It is generally accepted that anisotropy results from a balance between chemical etching and ion activated etching. Chemical etching most often results from reactions initiated by neutral radicals which arrive at the substrate isotropically and are adsorbed onto the surface. Such etching is characterized by a large degree of undercutting beneath the mask and fairly isotropic features. Ions arrive at the substrate with trajectories which are nearly normal to the surface and preferentially activate the etch on the horizontal bottom surfaces of the trenches, thereby producing anisotropic features. A polymeric film may also form on the walls of trenches and inhibit the isotropic chemical component of the etch. This process, known as side-wall passivation, is largely responsible for producing anisotropic features in many systems.² Since the isotropic flux of neutral radicals is typically much greater than the anisotropic flux of ions, isotropic etching would normally occur in the absence of such passivation.

The most commonly used tools for etching of semiconductors are parallel plate capacitively coupled radio frequency (rf) discharges.³ The generally accepted view of the precursors to etching generated in these systems is that the neutral radicals are in their ground state and have a Maxwellian distribution of kinetic energies, usually at some low temperature (300–600 K). Ground-state neutral radicals may carry a chemical potential to the substrate but

are assumed to deliver little translational or internal activation energy. Conversely, ions are somewhat chemically inert but are translationally energetic and carry significant activation energy to the substrate (10^2 – 10^3 eV/ion).⁴ There exist, however, processes in typical etching plasmas which can generate a substantial number of activated neutral species which, in turn, can deliver activation energy to the substrate. This energy is important because activated neutrals can arrive isotropically on the substrate and may initiate etching processes on sidewalls which would not otherwise occur, thereby degrading the anisotropy of the etch.

The presence of translationally hot neutrals may also be an important consideration in gas-phase chemical reactions. Gas-phase reaction rate coefficients can be quite temperature dependent, particularly those having an activation energy barrier. Processes having an activation barrier of greater than several kcal/mol have negligible rates if the reaction partners have Maxwellian velocity distributions with temperatures of 300–400 K. Such reactions could, however, be readily activated by the energy available in translationally hot neutrals. The effective rate coefficient in the presence of translationally hot neutrals could be orders of magnitude larger than the thermal value.

Similar considerations apply to reactions at the substrate. Consider the etching of silicon in a fluorocarbon plasma such as CF_4 . The sticking probability of a thermal F atom on a clean Si(100) surface is near unity. However, the silicon surface is typically passivated by a layer of adsorbed fluorine⁵ or fluorinated polymer, and the probability of sticking on a saturated surface is as low as 10^{-2} (Ref. 6). The preliminary data that is available for the energy dependence of the sticking probability of F on fluorinated Si indicates that sticking roughly doubles when the incident fluorine atom energy increases from 0.1 to 0.5 eV, and that the adsorption of atomic fluorine may be activated.⁶ In

this respect, translationally hot F atoms may be capable of breaching side-wall passivation.

In this paper we will theoretically examine the generation and consequences of translationally hot species resulting from dissociative excitation in etching discharges. The specific system we will consider is a parallel-plate rf CF_4 discharge, but the results are applicable to many etching system chemistries. The flux and energy spectra of these species are discussed using results from combined electron kinetics, plasma chemistry, and Monte Carlo models. We find that the flux of translationally hot neutrals onto the substrate is most important in discharges having pressures of $\approx 10\text{--}100$ mTorr. At low pressures (< 10 's mTorr), the flux of radicals may contain isotropic "beams" of nearly monoenergetic F atoms. This is particularly the case in low pressure (< 1 mTorr) remote plasma sources such as electron cyclotron resonance (ECR) devices.

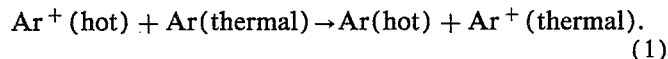
In Sec. II we will discuss important features of the production of hot atoms and their subsequent thermalization. In Sec. III we will describe the models we used analyzing transport of translationally hot neutrals, followed in Sec. IV by our predictions for their fluxes. Our concluding remarks are in Sec. V.

II. HOT ATOM PHYSICS AND CHEMISTRY

In this section we will discuss mechanisms responsible for the production of translationally hot neutrals, their subsequent transport through the discharge volume, and their possible effects on etching when they reach the substrate.

A. Production

There are at least four sources of translationally hot neutrals in etching discharges: charge exchange, reflection neutrals, dissociative recombination, and electron impact dissociation of molecules. In the first process, a hot neutral is generated in the sheath of a glow discharge when an energetic ion undergoes a charge exchange collision with a thermal neutral. For example,



This process is most important for symmetric charge exchange, as shown in Eq. (1), since for ion energies of < 10 's– 100 's eV cross sections for symmetric charge exchange are typically larger than those for asymmetric charge exchange.^{7–9} Since the differential cross section for charge exchange is strongly forward peaked with broadening largely determined by the thermal distribution of the target neutral, a hot neutral emerging from a charge exchange collision has a trajectory similar to that of the incident ion.¹⁰ The flux of translationally hot neutrals generated by charge exchange collisions in the sheaths is therefore dominantly anisotropic. The flux of hot charge exchange neutrals on the substrate may therefore differ little from ions in either energy distribution or their effect on etching. Since the distribution of these hot neutrals is similar to that of ions, their effects can be somewhat regulated in the same manner in which one controls the flux of

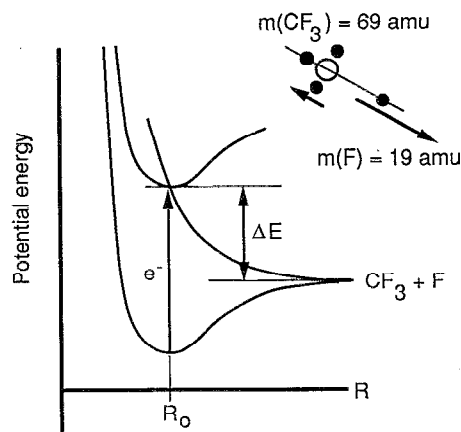


FIG. 1. Schematic of the potential energy surfaces accessed during the electron impact dissociation of a molecule such as CF_4 . Excitation of the upper electronic level crossing with a repulsive potential surface results in dissociation of the molecule. The fragments must then dissipate the excess energy ΔE , often in translational modes.

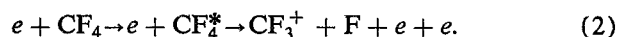
energetic ions (judicious choice of reactor geometry, rf voltage, and dc bias).

Reflection neutrals are hot atoms or molecules which recoil from the substrate after an energetic ion is neutralized. The energy distribution of these neutrals depends on the energy and type of ion incident on the substrate, and the condition of the surface. Hot atoms can also be generated as a result of dissociative recombinations of molecular ions. The mechanism is identical to that described below for electron impact dissociation. The relative rate of generation of hot atoms by this method increases with increasing fractional ionization. It makes a small contribution as long as $[e]/N$ (electron density/gas density) is $< 10^{-4}$.

The last source of translationally hot neutrals, and the only source we will consider in the remainder of this paper, is dissociative excitation of molecules by electron impact. In this process, schematically illustrated in Fig. 1, a molecule is initially excited to a higher electronic state. If a dissociative potential surface crosses that of the electronic state a spontaneous dissociation may occur. The excess energy ΔE may be dissipated by radiation or into the internal and translational modes of the fragments. If the transitional state is the lowest electronic state of the parent molecule, then dissipation of the excess energy by radiation or into the electronic states of the fragments is not likely. In this case dissipation is dominantly into the vibrational modes of the fragments or into translational energy. The photodissociation analog of this process has been used for many years to produce translationally energetic fragments to study hot atom chemistry.¹¹

In the electron impact dissociation of CF_4 into neutral fragments, the threshold energy is ≈ 12.5 eV (Ref. 12) and the $\text{CF}_3\text{—F}$ bond energy is ≈ 5.4 eV. This leaves a minimum of 7.1 eV to be dissipated in the dissociation process. Statistical theories predict that the excess energy will be equally partitioned into the translational and energetically accessible vibrational (and electronic) modes of the frag-

ments.¹³ Since the lifetimes of the transition states are typically short there may not be an opportunity for the partitioning to take place. A significant fraction of the energy may therefore be translationally dissipated. It is difficult to directly measure the energy of such hot neutral fragments. However, measurements have recently been made by Ce Ma, Bruce, and Bonham for the energy distribution of charged fragments emerging from the dissociative ionization of CF₄.¹⁴



They found that the average energy of the CF₃⁺ fragment released in the reaction shown in Eq. (2) is 1.6 eV with a FWHM of 0.8 eV for an electron impact energy of 20 eV. The F and CF₃⁺ fragments must preserve the initial (zero) linear momentum of the transition-state CF₄^{*}. Simple dynamics requires that the less massive F atom carry off most of the excess energy. We therefore infer that the F atom leaves the dissociation with 4–9 eV of translational energy. Under these conditions virtually all of the energy in excess of the appearance potential of CF₃⁺ is dissipated in translational modes. Measurements by Zukhov *et al.* for the electron impact dissociative ionization of O₂ and CO₂ indicate that the ion fragments leave the dissociation with energies up to ≈8 eV with a dominantly isotropic distribution for electron impact energies of 45–150 eV.¹⁵

For the purposes of further discussion in this paper, and as a demonstration system, we consider only dissociation of CF₄ into neutral fragments as the source of translationally hot neutrals. We note that for electron impact energies >30 eV, the rate of dissociative ionization exceeds that of dissociation into neutral fragments. Our assumptions will therefore tend to underestimate the true rate of production of hot neutrals. We also assume that the CF₃ fragment is produced in its ground state, requiring that all the excess energy be translationally dissipated. The initial F atom translational energy is taken to be 8 eV and the angular distribution to be isotropic (see Sec. III C 2). The exact launch energy does not substantially affect the results of our study because of the manner in which the hot F atoms slow is a smoothly varying function of energy, as discussed below.

B. Hot atom thermalization

Hot neutral atoms generated, for example, by electron impact dissociation are slowed by collisions with the background gas. The collisions may be elastic, result in excitation of the molecule, or may activate chemical reactions. Hot atom collisions, particularly those involving hot H atoms, have been studied in some detail and several reviews have been published.^{16,17} Most experiments, however, are unable to directly probe the details of the hot atom collision process, and the microscopic details of hot atom collisions must be inferred from hot atom kinetic theory.

Experiments by Baer and Amiel¹⁸ showed that the slowing of hot atoms (Br, Cl, H, and F) in an inert background gas (He, Kr, Ne, and Ar) can be explained by considering only elastic collisions, and that the thermalization process depends only upon the masses of the collid-

ing particles. Alfassi and Amiel¹⁹ later extended this theory to include inelastic processes by considering the internal and translational energies of the products resulting from a collision between a hot atom and the background gas. They concluded that inelastic energy transfer is less important for hot atom collisions with symmetric gas molecules such as CH₄, CF₄, and C₂H₆ because such molecules possess no permanent dipole moment. The hot atom therefore interacts with a weak induced rather than a strong permanent dipole. An extreme example is the interaction of hot F and SF₆, which is almost completely elastic in character.²⁰ As a result, SF₆ is commonly used as both a source of hot F atoms (from nuclear recoil reactions) and as a moderator to slowly thermalize energetic F atoms for hot atom chemistry experiments.^{16,17}

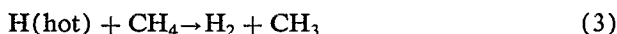
Alfassi and Amiel¹⁹ found that hot H atom reactions deviated somewhat from this prescription. They attributed the differences to the high translational speed of the light H atom relative to the more massive hot halogen atoms for a given kinetic energy. The duration of the H-molecule collision is sufficiently short that the H atom interacts with only a single atom in the molecule. A symmetric molecule such as CH₄ appears only as an asymmetric ≡C—H molecule to the passing H atom, in which case the collision has a substantial inelastic component.

The degree to which inelastic energy transfer affects a given collision process can be deduced by comparing the experimentally determined energy loss with that expected from kinetic theory under the assumption that all processes are elastic. The observed power loss for hot atoms in noble gases is consistent with elastic energy transfer, as are collisions in the F-SF₆, F-CH₄, F-CF₄, Cl-CH₄, Cl-C₂H₆, and Br-CH₄ systems.¹⁹ Deviations from pure elastic energy transfer may be a result of the high probability of hydrogen abstraction reactions by the incident halogen atom, particularly near thermal energies. Good agreement with experiment is obtained assuming elastic scattering in spite of there being a high probability of hydrogen abstraction. This may be a consequence of the energy of the halogen atom being similar after either an elastic collision or one in which an H atom is abstracted. Systems for which much of the energy transfer is inelastic in character are Cl-CH₃Cl, Cl-CH₃Br, and Br-CH₃Br.¹⁹

The F-CH₃CF₃ system has been studied in detail^{21,22} because it is similar to the fully halogenated alkanes (e.g., CF₄, CCl₄), but the reaction kinetics are more easily diagnosed. As might be expected in collisions between F atoms and target molecules having H atoms, there is a high probability that the F atom will abstract an H to form HF. There is also a strong tendency in the F-CH₃CF₃ system to form excited organic reaction products which subsequently decay by unimolecular decomposition. Whether excited reaction products decay by unimolecular decomposition or are collisionally stabilized is determined by the density of the background gas. We note that other hot atom systems of interest to the plasma processing community have also been studied, including Cl, Br, I, C, Si, S, P, and Ge.¹⁷

Abstraction is the most likely reaction channel for many hot atom-molecule systems.¹⁷ The abstraction pro-

cess is particularly important in hot H atom systems because the collision time in reactions such as



is similar to the vibrational period of the C—H bond. It is therefore likely that energy will be transferred into a single C—H bond and break it. The analogous process in F-CF₄ and other halogenated systems is an order of magnitude less likely for three reasons. First, the collision time is longer since a hot F is slower than a hot H having the same kinetic energy. Hence, there is more opportunity for collision energy to redistribute within the target molecule. Second, the bond energies are higher in the halogenated systems and may result in substantially lower reactivities. Third, steric hinderance may impede the larger halogen atoms.¹⁶

C. Hot atom processes in etching plasmas

In view of the preceding discussion, we have estimated that inelastic processes account for <10%–20% of the collisions between hot F atoms and CF₄. As discussed below, elastic interactions are the most frequent type of collision process, and because the collision partners have commensurate masses, elastic collisions are also the dominant energy loss process for hot F atoms. The details of the elastic collision depends on the potential energy surface between the hot atom and its collision partner. The Lennard–Jones 6-12 (LJ) potential is a simple but acceptably accurate form for the elastic interaction potential²³ and was used in this study. The LJ potential consists of a short-range repulsive term and long-range attractive term which leads to van der Waals bonding,

$$V(r) = 4\epsilon [(\sigma/r)^{12} - (\sigma/r)^6], \quad (4)$$

where V is the potential energy when the molecules are separated by a distance r . The free parameters σ and ϵ represent the range and depth of the potential, and were obtained from Refs. 24 and 25. The cross section for elastic collisions between neutrals resulting from the LJ potential has been addressed at length by others, and we refer the reader to Refs. 24 and 26 for details of the derivation. The cross section arising from the LJ potential can be reduced to a normalized form, as shown in Fig. 2. In normalized form the characteristic energy is $\epsilon_r = \frac{1}{2}\mu v_r^2/\epsilon$, where μ is the reduced mass of the collision pair, v_r is their relative speed, and ϵ is the LJ parameter.

We focus on two features of the normalized collision cross section. First, the cross section decreases monotonically with increasing energy. Translationally hot neutrals will therefore always have a longer mean free path than thermal neutrals. Second, the cross section varies rapidly at small ϵ_r . For gas temperatures significantly below room temperature or collision partners which have a large ϵ (corresponding to small ϵ_r), thermal energy corresponds to a point on the steeply sloped portion of the cross section. The increase in mean free path of hot atoms relative to that for thermal atoms will be particularly large for these systems. In F-CF₄ collisions $\epsilon/k=129$ K (k is Boltzmann's

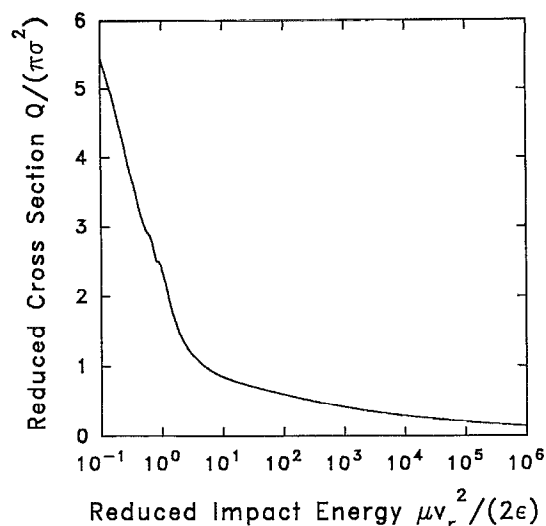


FIG. 2. Cross section corresponding to the Lennard–Jones 6-12 potential as a function of reduced collision energy, ϵ_r . Collisions between thermal neutral particles typically correspond to a reduced collision energy $\epsilon_r = 1-10$.

constant), whereas $\epsilon/k=358$ K for Cl-HCl collisions, another important etching chemistry. Hot atom effects are therefore more likely to be important in the latter system.

Collisions between hot neutrals and thermal molecules may result in vibrational excitation of the molecule. In virtually all systems of interest, however, vibrational excitation is unlikely to constitute a major channel for energy loss since many quanta of vibrational energy would need to be excited during every collision for the energy loss to compete with that due to elastic scattering. For example, the vibrational quanta in CF₄ is only hundreds of cm^{-1} , which represents a small energy loss per collision compared to the energy loss experienced in the average elastic collision. Energy transfer by hot atoms to vibrational excitation is therefore not included in our analysis. Energy lost to the excitation of rotational levels is much less than that for vibrational excitation, and also is not included. Electronic excitation of the molecule by hot atoms resulting from the dissociation process (≤ 10 eV) is similarly ignored in our analysis. Electronic excitation of the molecule is unlikely to occur because the momentum transfer between heavy neutrals and orbital electrons is poor, and in many cases is not energetically possible.

Chemical reactions between hot atoms and the background gas are entirely dependent upon the particular chemical system of interest. Abstraction is the most likely channel in many hot atom systems, though this process has a frequency of only a few to 20% of the rate of elastic collisions for F-CF₄.¹⁹ We can obtain a further estimate of the importance of this process from the temperature dependent reaction rate coefficient, κ , typically used for a Maxwellian distribution of speeds:

$$\kappa = AT^b \exp(-E_a/kT), \quad (5)$$

where A is the Arrhenius factor, E_a is the activation energy, and b is a constant. In cases where $b = \frac{1}{2}$ such as

F-CF₄ reactions, the preexponential factor $T^{1/2}$ can be assumed to be entirely due to the integration over the Maxwellian distribution function, and a cross section can be derived. For F-CF₄ reactions the Maxwellian averaged cross section for thermal energies is negligibly small; however, we estimate an abstraction cross section of $\approx 4.5 \text{ \AA}^2$ (Ref. 27) for atoms having energies greater than the activation energy (3.7 eV). The thermal cross section for elastic F-CF₄ collisions (found from the Lennard-Jones parameters) is an order of magnitude larger at $\approx 55 \text{ \AA}^2$. Hot atom reactions in the F-CF₄ system are therefore not important with respect to energy loss and can be ignored in the thermalization process. However, they may, in general, be important because they can generate reaction products which simply are not produced if all the neutrals were thermal.

In summary, hot F atoms slow dominantly by elastic collisions in CF₄, though inelastic collisions may be important with respect to the chemistry they initiate. Hot F atoms in CF₄ will generally thermalize after traveling a distance $\lambda \approx 10\lambda_{\text{HS}}$ from their launch point, where λ_{HS} is the mean free path expected from the low-energy hard-sphere collision cross section. The factor of 10 comes from the observations that hot atoms lose on the average approximately one-third of their energy in each elastic collision with the fill gas depending on the exact nature of the differential scattering cross section, and that the mean free path for hot neutrals is typically three times that for thermal neutrals.

III. DESCRIPTION OF THE MODEL

In this section, we will describe our models for transport of hot atoms in etching plasmas. Our demonstration system is hot F atoms in rf discharges sustained in CF₄. Our simulation for the transport of translationally hot F atoms consists of two linked models. The first is a model of the electron kinetics in the etching plasma from which we obtain the production rate of hot F atoms resulting from electron impact dissociation of CF₄. In the second model the trajectories of the hot atoms are followed as they slow in the gas.

The transport and slowing of hot atoms was modeled using a Monte Carlo simulation (MCS). In this portion of the model, hot F atoms are launched from preselected positions in the plasma with an isotropic velocity distribution. These launch locations are evenly spaced between the electrodes when modeling parallel plate discharges. The distance d to the next collision is chosen from $d = -\lambda(\epsilon') \ln(r)$, where r is a random number evenly distributed on $[0, 1]$, and $\lambda(\epsilon')$ is the mean free path of the hot neutral based on energy ϵ' . The energy-dependent mean free path was obtained from the cross section derived from the LJ potential as described above and the density of the background gas. The straight line trajectory of each atom is recorded for the distance d before the collision. The angular distribution of the hot neutral after scattering is assumed to be that given by hard-sphere dynamics, $\theta = 2 \cos^{-1}(r)$. This latter assumption most likely underestimates the range of very hot atoms since at high energies

the differential cross section is likely to be more forward peaked. It is, however, a reasonable approximation to the distribution for kinetic energies $> 10\epsilon$, typically a few tenths eV.^{24,26} Below this energy, significant backscattering occurs and the forward-scattering approximation is no longer valid. The momentum transfer in the collisions is governed by classical elastic collision theory, yielding a momentum change during the collision of

$$\frac{\Delta p_i}{p_i} = \frac{m_i}{m_i + m_t} \cos(\theta) \pm \left[\left(\frac{m_i}{m_i + m_t} \right)^2 \cos^2(\theta) + \frac{m_t - m_i}{m_i + m_t} \right]^{1/2} - 1, \quad (6)$$

where m_i and m_t are the masses of the incident and target particles, θ is the angle between the initial and final velocity vectors of the incident particle, and p_i is the momentum of the incident particle. If $m_i > m_t$ then $\theta < \theta_m$, where $\cos^2 \theta_m = 1 - (m_t/m_i)^2$ and $0 \leq \theta_m \leq \pi/2$.

The result of this portion of the model is a relation resembling a Green's function $p(z, \epsilon_i, \epsilon_f, \theta)$, where p is the probability that a hot neutral launched at a distance z from the substrate with energy ϵ_i will impact the substrate with energy ϵ_f and angle θ for normal incidence. This probability is invariant for a given gas mixture and electrode spacing. The spectrum of hot neutrals striking the substrate $F(\epsilon_f, \theta)$ is then found by convolving the spatially dependent rate of production of hot neutrals having energy ϵ_i , $R(z, \epsilon_i)$, with the Green's function

$$F(\epsilon_f, \theta) = \int_0^{\epsilon_{\text{max}}} \int_0^L R(z, \epsilon_i) p(z, \epsilon_i, \epsilon_f, \theta) dz d\epsilon_i. \quad (7)$$

We have allowed for a distribution of launch energies in this formulation, which could result from a statistical redistribution of energy in the parent molecule prior to fragmentation.

The production rate of hot F atoms, $R(z, \epsilon_i)$, is obtained from a hybrid model for the electron kinetics in a rf discharge. Hot F atoms are assumed to originate exclusively from the electron impact dissociation of CF₄ into CF₃ + F, the neutral analog of Eq. (2). The branching ratios for neutral fragments resulting from electron impact dissociation are not well known. Plumb and Ryan estimated that the branching to CF₂ + 2F has a 0.7 probability while that to CF₃ + F has a 0.3 probability.²⁸ The branching for dissociative ionization to CF₃⁺ + F for electron energies < 100 eV, though, exceeds 0.7.¹⁴ We have assumed that the F atoms emerge from the dissociation with fixed energy of $\epsilon_i = 8$ eV. We have therefore implicitly assumed that all of the CF₃ reaction product is produced in its ground state and that the predissociative electronic state to which the CF₄ is excited is near the ionization limit. Results from Ma, Bruce, and Bonham¹⁴ indicate that the F atom is actually produced with a range of energies from 4 to 9 eV. The precise value of the launch energy does not qualitatively alter the algorithms or results of this study provided that the launch energy is greater than thermal. This condition results from elastic collisions being the

dominant mode of slowing and the assumption that other collision channels are not opened by higher launch energies.

The hybrid electron kinetics model consists of a semi-analytic model for the sheaths combined with a Monte Carlo simulation of the electron trajectories (eMCS). Given a specified form for the time and spatially varying electric fields in the discharge, the eMCS follows the trajectories of the electrons over many rf cycles, including the appropriate collisions for momentum transfer and energy loss. The result of the eMCS is the electron energy distribution (EED) as a function of position and phase during the rf cycle. Rates for the various electron impact processes as a function of space and time (z, t) can then be obtained from the EED. The second component of the hybrid model is a macroscopic model from which the electric fields in the rf discharge are obtained for input to the eMCS. The macroscopic model is based on the works of Misium *et al.*²⁹ and Godyak and Sternberg.³⁰

The basis of the eMCS model has been previously reported^{31,32} and therefore will be only briefly described here. The simulation begins with a user-specified form for the electric fields in the discharge. The assumed fields have a linear spatial dependence in the sheaths and are spatially invariant in the bulk plasma. The applied voltage is then oscillated in time at the rf frequency and electron trajectories calculated. Particle densities are recorded as a function of position and time to generate the electron energy distribution. The rate coefficients for elastic, excitation, ionization, and dissociation collisions are then found by convolving the distribution function with the appropriate cross section. Electron impact cross sections for CF₄ were obtained from the compilation by Hayashi,³³ and were used without further modification.

The rates calculated in the eMCS are then used as input to a macroscopic model based largely on work of Misium *et al.*²⁹ This model is simplified by our assumption that no electrons are released from the electrodes by ion impact. The macroscopic model produces a time-averaged sheath length which is returned to the eMCS. The bulk electric field amplitude, which is also returned to the eMCS, is found by assuming that the electrons carry the total discharge current at the midplane of the plasma. The field is then specified by using the discharge current predicted by the macroscopic model and the electron mobility obtained from the eMCS. The presheath was presumed to begin at the location where $\bar{E} = T_e/\lambda_D$,³⁰ where \bar{E} is the time-averaged field, T_e is the electron temperature (from the eMCS), and λ_D is the Debye length at the same location.

We expect that this hybrid model will accurately predict trends in a rf discharge, but because it is not totally self-consistent with respect to electric fields, there are some deficiencies. The macroscopic model assumes one dominant positive ion species and therefore does not properly handle the negative ions arising from electron attachment processes. We do not believe this to be a serious problem because the electric field predicted by the macroscopic model is based on the electron energy balance which is not

dramatically influenced by the presence of negative ions. The macroscopic model is known to underestimate the power deposition due to electron heating resulting from sheath motion.^{29,34} The utility of the hybrid model is in its speed of execution and its ability to predict qualitative trends as discharge parameters (e.g., voltage and gas pressure) are varied. Since the parameters of interest for this study are the spatial distributions of electron impact dissociation and ionization collisions, values which are accurately predicted by the eMCS, we expect the weaknesses of the hybrid model to be of secondary importance.

IV. HOT ATOMS IN PARALLEL-PLATE rf AND ECR DISCHARGES

In this section we will discuss the energy spectra of hot atoms in rf discharges with emphasis on their likely effects on etching processes.

A. Energy spectra and fluxes in rf discharges

The spatially dependent rate of electron impact dissociation calculated for a parallel-plate discharge is shown in Fig. 3(a) for CF₄ at 10 and 100 mTorr. The applied voltage is 400 V (13.56 MHz) and the electrode separation $L = 5$ cm. Similar values are shown for 30 mTorr at potentials of 300–500 V. The rate of dissociation has a maximum near the edge of the sheaths, a result of the sheaths oscillating which generates high-energy electrons there. The maximum in the rate of production is displaced toward the center of the discharge at lower pressures and higher voltages, a reflection of the thicker sheaths for those conditions.

Assuming that each dissociation produces one isotropically emitted hot F atom with 8 eV of translational energy, the spectrum of F atoms incident on either electrode is shown in Fig. 4 for CF₄ pressures of 10, 30, and 100 mTorr. For these results, and those that follow, the F atoms are tracked from their site of production to their first strike on the electrodes. The reflection and desorption of F atoms from the surface are not considered. At low gas pressures (10 mTorr), many of the energetically produced F atoms stream through the discharge without colliding and reach the substrate with their full launch energy. As the neutral pressure is increased, the hot F atoms undergo more collisions with the background CF₄ and reach the substrate with a more thermalized distribution. The spectra have two prominent peaks resulting from hot atoms which reach the substrate without collisions and those which have collided many times and have been thermalized. The structure in the energy spectra between the hot and thermalized peaks is reproducible, but is sensitive to the details of the cross section and scattering angles. The precise form of this structure is not important with respect to our conclusions.

The fraction of F atoms which are nonthermal when they reach the substrate is plotted in Fig. 5 as a function of gas pressure for different applied voltages. The nonthermal fraction increases with decreasing gas pressure because the hot atoms undergo fewer energy loss collisions. The fraction of neutrals which strike the surface with energies sig-

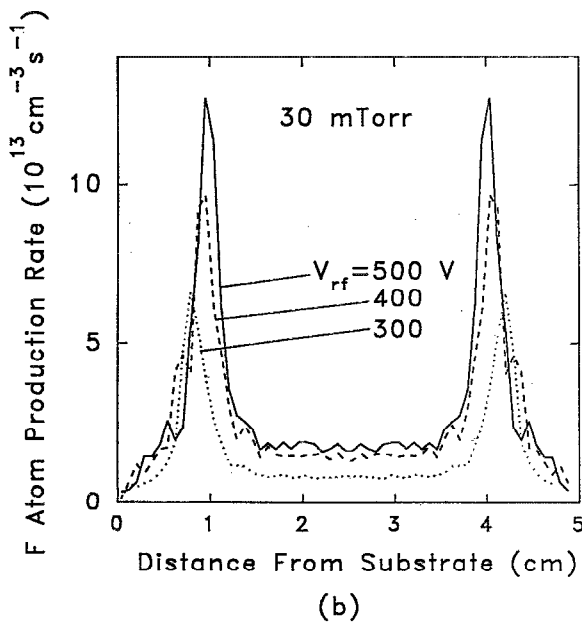
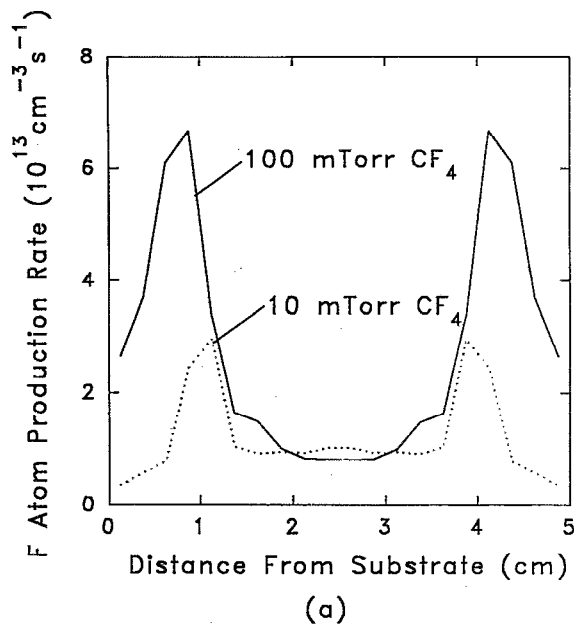


FIG. 3. Spatial profile of the time-averaged rate of electron impact dissociation of CF_4 for (a) an applied voltage amplitude of 400 V at gas pressures of 10 and 100 mTorr, and (b) various voltages for 30 mTorr. The electrode separation is 5 cm. The source moves away from the substrate as low pressures and higher voltages due to the thickening of the sheaths.

nificantly above thermal energy nears unity for pressures < 10 mTorr and is negligible for pressures > 100 's mTorr. The nonthermal fraction is relatively insensitive to operating voltage at lower pressures. The fractional flux of hot atoms incident on the surface does not depend on the magnitude of the source of atoms but the distance of the source from the substrate Λ and the gas pressure p . As $p\Lambda$ increases, the nonthermal flux decreases. The $p\Lambda$ product increases with increasing voltage since the sheath thickness

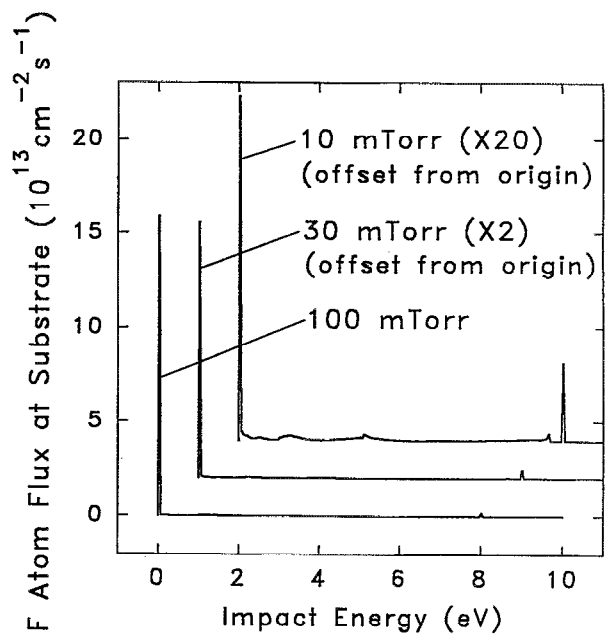


FIG. 4. Spectra of hot F atoms arriving at the substrate having launch energies of 8 eV. The source functions are as given in Fig. 3. The spectra consist dominantly of ballistic hot atoms arriving at the substrate without collisions and fully thermalized atoms.

increases somewhat and the average location of production moves away from the substrate. The nonthermal fraction increases slower than one might otherwise expect with decreasing pressure because the source of hot F atoms moves away from the substrate at lower pressures as the thickness of the sheath increases (see Fig. 3).

The volume-averaged production rates for hot F atoms as a function of gas pressure and voltage are shown in Fig. 6. The total production rate of hot atoms increases with increasing gas pressure because a larger fraction of the

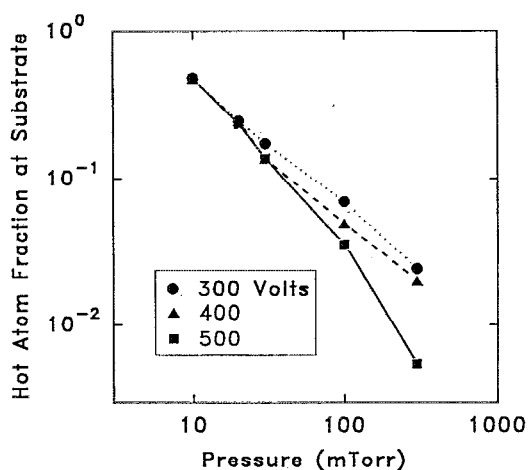


FIG. 5. Fraction of F atoms arriving at the substrate which are nonthermal as a function of CF_4 pressure. An F atom with less than 0.05 eV is defined as being thermal, though the results are not sensitive to this definition. At pressures less than 10's of mTorr, the flux of F atoms is dominantly nonthermal.

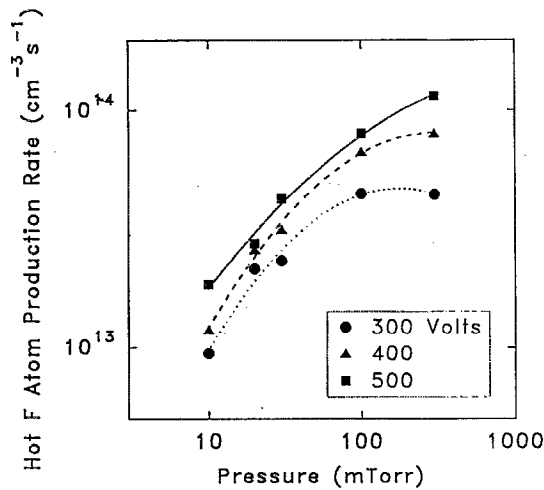


FIG. 6. Rate of production of hot F atoms as a function of gas pressure and voltage averaged over the volume of the discharge. The production rate increases with increasing gas pressure due to the larger proportion of discharge power dissipated by electron collisions.

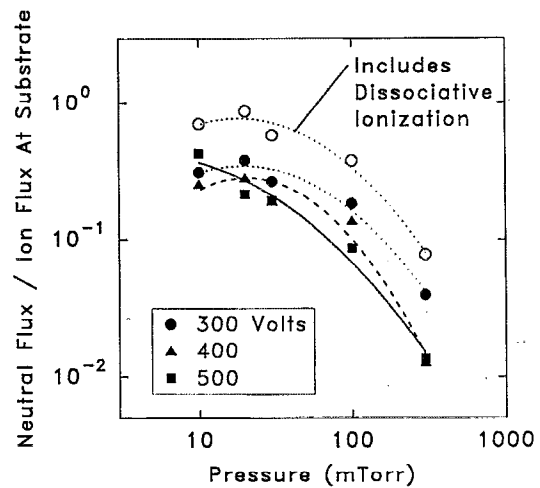


FIG. 8. Nonthermal neutral flux at the substrate expressed as a fraction of the incident ion flux. The nonthermal atom flux can be commensurate with the ion flux at low pressures. The increase in the hot atom flux which may occur when including those generated by dissociative ionization is also shown.

discharge power is dissipated by electron collisions as opposed to ion bombardment of the electrodes. The production rate increases with increasing voltage since the absolute power deposition also increases. The absolute fluxes of nonthermal F atoms striking the substrate are shown in Fig. 7 for the same conditions. In deference to the production rates, the total hot atom flux striking the substrate generally decreases with increasing pressure due to the increase in $p\Lambda$. The flux begins to decrease at low pressure due to the fall-off in the rates of production. A weak maximum may then occur in the nonthermal flux for pressures of 10's mTorr to 100 mTorr.

The gas pressure at which the nonthermal flux is maximum and the relative magnitude of the maximum are

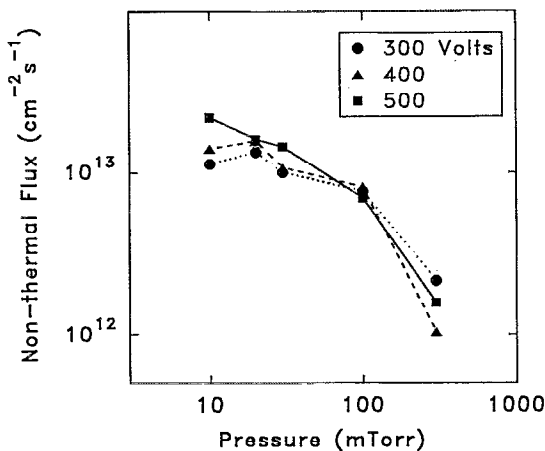


FIG. 7. Nonthermal flux of F atoms incident on the substrate as a function of voltage and pressure. The flux has a weak maximum at pressures of 10's of mTorr resulting from an increase in the rate of production of hot F atoms and decrease in their flux as the gas pressure increases. Results are also shown for including hot atoms from dissociative ionization.

quite sensitive to the details of the thickness of the sheath and the collision cross section. The pressure and magnitude of the maximum have important implications on processing "windows" and may vary from system to system. At low gas pressures (< 10 's mTorr), the hot atom flux depends primarily upon the total hot atom production rate, since for these conditions, the hot atoms stream nearly collisionlessly to either electrode. At high fill pressures (> 300 mTorr), hot F atoms undergo many collisions before striking the substrate. In this regime the hot neutral flux to the substrate is sensitive to the production rate within a few hot neutral mean free paths of the substrate. While in general higher voltages imply more dissociation because of the higher-power deposition, the sheaths are also somewhat thicker at higher voltages. The spatial maximum in the production rate moves away from the substrate, thereby allowing more collisions to occur before the hot flux strikes the electrodes. At intermediate gas pressures (many 10's-100's mTorr) the effects of increasing production rate and increasing $p\Lambda$ with increasing pressure or voltage may conspire to produce a maximum in the hot atom flux striking the substrate. At these pressures, the thermalization distance for hot F atoms and Λ (the distance from the substrate to the peak in the production) are comparable.

The flux of nonthermal F atoms at the substrate is important in etching plasmas because it may increase the isotropic component of the etch. A measure of this effect is the ratio of the hot atom flux to the ion flux striking the substrate. This ratio is plotted in Fig. 8. The hot atom flux is comparable to the ion flux at intermediate gas pressures, and is still 1%-10% of the ion flux at pressures exceeding 100's mTorr. The ratio is smaller at higher voltages due to the increase in the rate of ionization compared to neutral dissociation. Including the additional hot F atoms which may be produced during dissociative ionization, the ratio may exceed unity at low pressures, as shown in Fig. 8. If

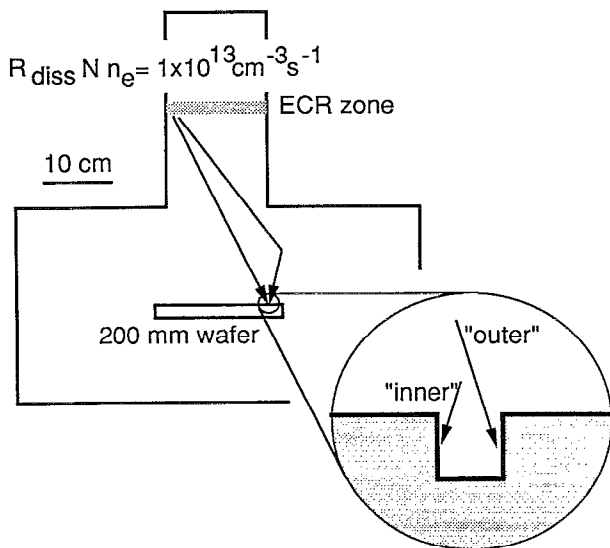


FIG. 9. Schematic of an electron cyclotron resonance (ECR) reactor as used in this study. The source region is assumed to be a 1-cm-thick disk at the ECR zone. The neutral dissociation rate within this zone was estimated to be $10^{13} \text{ cm}^{-3} \text{ s}^{-1}$. Hot atoms are assumed to thermalize upon striking a wall.

we assume hot neutrals and ions are equally likely to activate the etching process, the isotropic component could be 10's of percent for gas pressures of 10's of mTorr. An isotropic etch rate which is only a few percent of the vertical etch rate may be problematic if the desired etch product has a high aspect ratio (deep and narrow).

B. Low-pressure ECR reactors

Although the flux of hot atoms may saturate and begin to decrease with decreasing gas pressure, their fractional contribution to the total neutral flux always increases. Their increasing importance results from the fact that they arrive at the substrate isotropically and begin to compete with ions in determining the character of the etch. As shown above, the radical flux in low-pressure reactors may, in fact, be composed primarily of hot atoms. To illustrate the consequences of these conditions, we examined the flux of hot F atoms that may be produced in an electron cyclotron resonance (ECR) etching reactor. Such remote plasma systems are of interest because it is possible to obtain high electron densities (10^{11} – 10^{12} cm^{-3}) at low gas pressures ($< 1 \text{ mTorr}$).³⁵ These conditions are precisely those which result in a large flux of translationally hot neutrals reaching the electrode surfaces.

For this discussion we consider an idealized ECR source with the electron impact processes (excitation, ionization, and dissociation) confined to a 1-cm-thick region centered on the ECR resonance point. (See Fig. 9.) The ions diffusing out of the source region can be controlled by manipulating the magnetic fields applied to the plasma and the potential of the substrate. Neutrals are unaffected by such fields and, if the fill gas pressure is low ($< 1 \text{ mTorr}$), will radiate isotropically from the source region and travel

virtually collisionlessly to the walls of the reactor. The result is that the hot atom flux striking the walls of a trench depends in large part on the solid angle of the source viewed from that wall. Vertical surfaces facing outward generally view a smaller solid angle of the source than vertical surfaces facing inward. One therefore might expect that there will be a greater hot neutral flux to the wall of the trench nearest to the outer edge of the wafer relative to the flux seen by the wall nearest the center of the wafer. Barrelling of trenches has been observed in ECR systems and is generally attributed to the diverging magnetic field at the substrate and nonzero ion temperature. Hot neutrals may produce similar profiles when the source region is confined to the resonance zone if the higher flux of hot neutrals on the outer walls results in a higher etch rate. At very low pressures these effects may be mitigated because electron impact dissociation extends beyond the resonance zone toward the substrate.

We calculated the hot atom flux incident on the inner and outer walls of a trench on the substrate of our idealized ECR reactor and the results are shown in Fig. 10(a). We assumed that the dissociation rate in the ECR zone is $10^{13} \text{ cm}^{-3} \text{ s}^{-1}$ at 0.1 mTorr. Atoms which strike the walls are assumed to thermalize. We used two scalings: the source being constant as a function of pressure and the source scaling with pressure. The hot atom flux striking the outer wall monotonically decreases with increasing pressure due to there being more thermalizing collisions. The hot atom flux to the inner wall has a maximum corresponding to hot atoms having only a few collisions to redirect them to the inner surface, but not so many collisions that they thermalize. The ratio of the flux to the inner and outer walls approaches unity as the pressure increases and the flux becomes more randomized, as shown in Fig. 10(b).

C. Extension to other systems

As long as elastic collisions are the dominant energy loss process for hot neutrals, the results we have discussed here are somewhat insensitive to the gas mixture. The reason is that the Lennard-Jones parameters governing the collision cross sections do not vary by more than a factor of 2–3 for the gases of interest. The ϵ parameter varies more widely, but since the neutral temperature usually corresponds to a point on the flat portion of the cross section shown in Fig. 2, the cross section will depend only moderately on ϵ . The effects of the sharp increase in the cross section occur for $\frac{1}{2} \mu v^2 / \epsilon < 1$ and become apparent only for systems with very large ϵ or when the neutral gas temperature is substantially below room temperature. This could be problematic in systems using low substrate temperatures as are now being investigated.³⁶

D. Processes activated by hot neutrals

We have noted instances where the hot neutral flux is comparable to the ion flux to the electrodes, particularly at low pressures. Relatively small changes in the operating point in applied voltage or pressure can significantly reduce

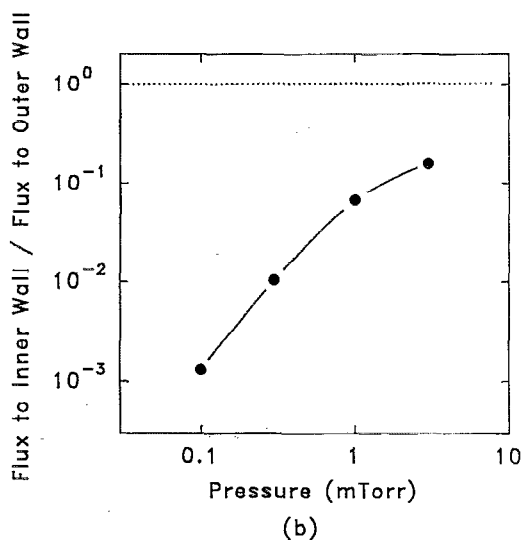
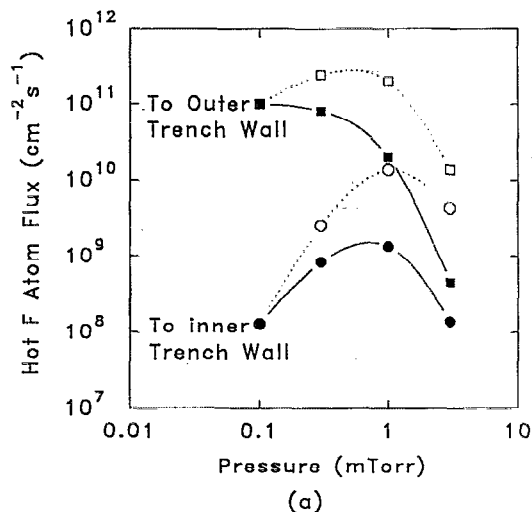


FIG. 10. Absolute flux of hot atoms to the "inner" and "outer" faces of a trench 8 cm from the center of the substrate. The open symbols denote a production rate of $1 \times 10^{13} \text{cm}^{-3} \text{s}^{-1}$ at 0.1 mTorr and which is proportional to fill gas pressure, while the filled symbols assume a production rate of $1 \times 10^{13} \text{cm}^{-3} \text{s}^{-1}$ for all pressures. (a) Total flux and (b) ratio of the flux to the inner and outer walls. The hot neutral flux striking the "inner" and "outer" walls of trenches at the edge of the substrate are disparate at low pressures, and begin to equilibrate at pressures exceeding a few mTorr.

or increase the hot atom flux, and so the rate of processes in which hot atoms participate are equally as sensitive. The most important of these processes are those which have activation energies sufficiently high that their rate of occurrence is negligible at thermal energies. Hot atoms represent an isotropic source of energetic particles at the substrate which may etch as effectively as the directed energetic ion flux. In addition, hot atoms may serve to activate gas-phase chemistry and produce gas-phase species which would otherwise not exist. Unique surface chemistry may be similarly activated by the energy available in hot neutrals; such threshold effects may be the most dramatic manifestation of hot neutrals. It is beyond the

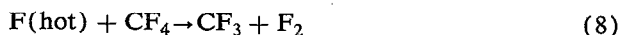
scope of this paper to investigate the specifics of a variety of chemical systems, but we can illustrate these points by example.

Measurements of the sticking coefficient of F on Si(100) over a large range of F atom energies have not been made, but there is evidence that the process is activated. F atoms stick with near unit efficiency on clean Si surfaces, but the sticking coefficients falls to 10^{-2} – 10^{-4} once the surface has been covered with a few monolayers of adsorbed fluorine. Engstrom *et al.*⁶ found that the sticking coefficient increases by $\approx 50\%$ when the translational energy of F incident on a Si(100) surface at 120 K is raised from 0.1 to 0.5 eV. If this scaling prevails to higher energies, one should expect at least an order of magnitude higher sticking coefficient at 10 mTorr compared to 100 mTorr. This increase in sticking, and implied reactivity, of F atoms on passivated surfaces could compromise the protecting nature of sidewall polymerization.

Many surface processes require the formation of an intermediate "precursor" state. Translationally hot neutrals may obviate the need for such an intermediate state because they carry sufficient energy to directly activate the process. Such "direct" processes will also be insensitive to the substrate temperature, thereby removing temperature as a useful control parameter of the surface process. Retner *et al.* have found just such an effect in the chemisorption of N_2 on W(100) and its subsequent dissociation.³⁷

Gas-phase collision processes may also be activated by hot neutrals. Gas-phase reactions which have an activation energy barrier of more than a few kcal/mol are typically not important in etching plasmas since the gas temperature is < 400 K. Since an activation barrier of 1 kcal/mol corresponds to approximately 0.05 eV, hot neutrals are easily able to activate such processes. The effect is particularly important for reactions which have sufficiently high activation energies that the process simply does not occur at processing temperatures.

We chose as an example the abstraction reaction



because for many hot atom chemistries abstraction is the most likely inelastic collision channel for impact energies of < 10 eV. The activation barrier of 86 kcal/mol. The rate of production of CF_3 by electron impact will be large relative to that by hot F atoms. Abstraction reactions, though, may be a significant source of F_2 , particularly at low pressure where association reactions are not easily stabilized, or a significant gas-phase loss for F atoms. The effective rate coefficient and absolute rate of production for this process as a function of gas pressure are shown in Fig. 11. The effective rate coefficient, k_e , is defined so that the total abstraction rate per unit volume is $k_e[\text{F}][\text{CF}_4]$, where $[\text{F}]$ is the total F density including thermal atoms. The effective rate coefficient monotonically increases with decreasing gas pressure due to the increase in the proportion of hot F atoms. The total rate of abstraction, though, has a maximum as a function of pressure.

The similarity of neutral-neutral collision processes as described by the Lennard-Jones potential may hinder at-

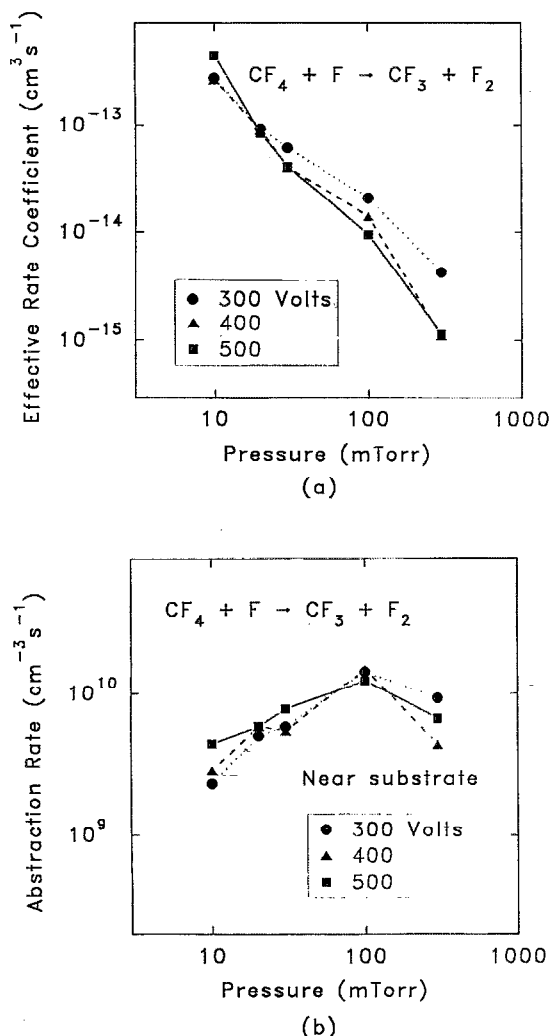


FIG. 11. Characteristics of hot atom activated chemistry. (a) The effective rate coefficient for the abstraction reaction $\text{F} + \text{CF}_4 \rightarrow \text{CF}_3 + \text{F}_2$ is shown near an electrode surface. (b) The absolute rate for the abstraction reaction $\text{F} + \text{CF}_4 \rightarrow \text{CF}_3 + \text{F}_2$ is shown as a function of gas pressure near the electrodes. The rate coefficient increases with decreasing density due to the increase in the nonthermal flux.

tempts to control translationally hot neutrals in etching discharges. The primary avenue available for modification of the hot neutral flux at the electrodes is to change the gas pressure or gas temperature. Unfortunately, large variations in any of these operating parameters will have only modest effects on the hot neutral flux to the substrate as long as hot atoms are slowed primarily in elastic collisions with the fill gas. One might also choose a chemistry which intrinsically generates a small flux of hot atoms. A carefully chosen chemistry may also be used to scavenge hot atoms from the discharge volume before they strike the substrate.

V. CONCLUDING REMARKS

Recent experimental results suggest that translationally hot F atoms having kinetic energies from several to 10 eV are produced in electron impact dissociation of CF_4 . Previous studies of hot atom transport have shown that hot

F atoms are relatively inert and do not appreciably react with a CF_4 background gas. They instead are primarily slowed by elastic collisions with CF_4 . Results from our models show that at moderate gas pressures (10–100 mTorr) the hot F atom flux at the discharge electrodes can be comparable to the ion flux. At lower gas pressures, the F atom production rate is reduced, while at higher fill gas pressures the hot F undergoes more moderating collisions with the CF_4 and is thermalized before reaching the discharge walls. High-power, low-pressure devices such as electron cyclotron resonance reactors are examples of reactors where the hot atom flux might be particularly large. Only fragmentary data exists on the effects of activated neutrals upon striking a surface. It is reasonable to expect that surface reaction and sticking rates will be enhanced by the activation energy available in such species, and measurements of the sticking coefficient of F on Si(100) tend to support this conjecture. Endothermic gas-phase reactions are also enhanced by the hot atom flux.

The production mechanisms and effects of translationally hot neutrals in etching discharges are still largely unknown. We have presented some general scaling laws which should be considered in the design or analysis of etching processes. Comprehensive models which address the issues discussed here will necessarily be sophisticated and must include the kinetics of the charged species, neutral gas-phase species, and surface reactions.

ACKNOWLEDGMENTS

The authors would like to thank M. S. Barnes, R. Buss, F. F. Crim, T. Engel, R. Iyer, J. Keller, E. J. Mansky, J. O'Neill, J. Singh, and H. F. Winters for their comments and guidance. R. Bonham kindly provided us with his results prior to publication. The authors would also like to thank the reviewer for his careful reading and comments. This work was supported by IBM East Fishkill Facility, the National Science Foundation (ECS88-15781 and CBT88-03170), and the Semiconductor Research Corporation.

- ¹D. M. Manos and D. L. Flamm, *Plasma Etching* (Academic, Boston, 1989), and references therein.
- ²M. Mieth and A. Barker, *J. Vac. Sci. Technol. A* **2**, 629 (1983).
- ³L. E. Kline and M. J. Kushner, *Crit. Rev. Solid State Mater. Sci.* **16**, 1 (1989).
- ⁴J. Liu, G. L. Huppert, and H. H. Sawin, *J. Appl. Phys.* **68**, 3916 (1990).
- ⁵D. L. Flamm, V. M. Donnelly, and M. A. Mucha, *J. Appl. Phys.* **52**, 3633 (1981).
- ⁶J. R. Engstrom, M. M. Nelson, and T. Engel, *Surf. Sci.* **215**, 437 (1989).
- ⁷H. W. Ellis, R. Y. Pai, E. W. McDaniel, E. A. Mason, and L. A. Viehland, *At. Data Nucl. Data Tables* **17**, 177 (1976).
- ⁸R. J. Shul, R. Passarella, B. L. Upschulte, R. G. Keese, and A. W. Castleman, *J. Chem. Phys.* **86**, 4446 (1987).
- ⁹A. V. Phelps, *J. Phys. Chem. Ref. Data* **19**, 653 (1990).
- ¹⁰D. Gerlich, *J. Chem. Phys.* **90**, 127 (1989).
- ¹¹G. W. Flynn and R. E. Weston, *Ann. Rev. Phys. Chem.* **37**, 551 (1986).
- ¹²H. Winters and M. Inokuti, *Phys. Rev. A* **25**, 1420 (1982).
- ¹³D. M. Mintz and T. Baer, *J. Chem. Phys.* **65**, 2407 (1976).
- ¹⁴C. Ma, M. R. Bruce, and R. A. Bonham, *J. Chem. Phys.* (to be published).
- ¹⁵A. I. Zhukov, A. N. Zavilopulo, A. V. Snergursky, and O. B. Shpenik,

- J. Phys. B **23**, 2373S (1990).
- ¹⁶R. Wolfgang, *Progr. React. Kin.* **3**, 97 (1965).
- ¹⁷T. Tominaga and E. Tachikawa, *Modern Hot-Atom Chemistry and its Applications* (Springer, Berlin, 1981).
- ¹⁸M. Baer and S. Amiel, *J. Chem. Phys.* **53**, 407 (1970).
- ¹⁹Z. B. Alfassi and S. Amiel, *J. Chem. Phys.* **57**, 5085 (1972).
- ²⁰R. L. Williams and F. S. Rowland, *J. Phys. Chem.* **77**, 301 (1973).
- ²¹K. A. Krohn, N. J. Parks, and J. W. Root, *J. Chem. Phys.* **55**, 5771 (1971).
- ²²K. A. Krohn, N. J. Parks, and J. W. Root, *J. Chem. Phys.* **55**, 5785 (1971).
- ²³R. B. Bernstein, *Atom-Molecule Collision Theory, A Guide for the Experimentalist* (Plenum, New York, 1979).
- ²⁴J. O. Hirschfelder, C. F. Curtiss, and R. B. Bird, *Molecular Theory of Gases and Liquids* (Wiley, New York, 1954).
- ²⁵R. A. Svehla, NASA Technical Report R-132 (1962).
- ²⁶J. O. Hirschfelder, R. B. Bird, and E. L. Spatz, *J. Chem. Phys.* **16**, 968 (1948).
- ²⁷A. P. Modica and S. J. Sillers, *J. Chem. Phys.* **48**, 3282 (1968).
- ²⁸I. C. Plumb and K. R. Ryan, *Plasma Chem. Plasma Process.* **6**, 205 (1986).
- ²⁹G. R. Misium, A. J. Lichtenberg, and M. A. Lieberman, *J. Vac. Sci. Technol.* **7**, 1007 (1989).
- ³⁰V. A. Godyak and N. Sternberg, *Phys. Rev. A* **42**, 2299 (1990).
- ³¹M. J. Kushner, *J. Appl. Phys.* **54**, 4958 (1983).
- ³²M. J. Kushner, *IEEE Trans. Plasma Sci.* **PS-14**, 188 (1986).
- ³³M. Hayashi, in *Swarm Studies and Inelastic Electron-Molecule Collisions*, edited by L. C. Pitchford, B. V. McKoy, A. Chutjian, and S. Trajmar (Springer, New York, 1987), p. 167.
- ³⁴C. G. Goedde, A. J. Lichtenberg, and M. A. Lieberman, *J. Appl. Phys.* **64**, 4375 (1988).
- ³⁵J. Hopwood, D. K. Reinhard, and J. Asmussen, *J. Vac. Sci. Technol. A* **8**, 3103 (1990).
- ³⁶S. Tachi, K. Tsujito, and S. Okudaira, *Appl. Phys. Lett.* **52**, 616 (1988).
- ³⁷C. T. Rettner, E. K. Schweizer, and H. Stein, *J. Chem. Phys.* **93**, 1442 (1990).